Published in final edited form as:
J Leukoc Biol. 2007 September ; 82(3): 465–476.

Pivotal Advance: Slit-2/Robo-1 modulates the CXCL12/CXCR4-induced chemotaxis of T cells

Anil Prasad[*], **Zahida Qamri**[*], **Jane Wu**[†], and **Ramesh K. Ganju**[*,1]

[*] *Division of Experimental Medicine, Beth Israel Deaconess Medical Center, Harvard Medical School, Boston, Massachusetts, USA*

[†] *Northwestern University Feinberg Medical School, Robert H. Laurie Comprehensive Cancer Center, Center for Genetic Medicine, Chicago, Illinois, USA*

Abstract

Slit, which mediates its function by binding to the Roundabout (Robo) receptor, has been shown to regulate neuronal, dendritic, and leukocyte migration. However, the molecular mechanism by which the Slit/Robo complex inhibits the migration of cells is not well defined. Here, we showed that Slit-2 can inhibit the CXCL12-induced chemotaxis and transendothelial migration of T cells and monocytes. We observed that CXCR4 associates with Robo-1 and that Slit-2 treatment enhances this association with the Robo-1 receptor. Robo-1 is a single-pass trans-membrane receptor whose intracellular region contains four conserved motifs designated as CC0, CC1, CC2, and CC3. Structural and functional analyses of Robo receptors revealed that interaction of the CC3 motif with the CXCR4 receptor may regulate the CXCL12-induced chemotaxis of T cells. We further characterized Slit-2-mediated inhibition of the CXCL12/CXCR4 chemotactic pathway and found that Slit-2 can block the CXCL12-induced activation of the Src and Lck kinases but not Lyn kinase. Although Slit-2 did not inhibit the CXCL12-induced activation of MAPKs, it did inhibit the Akt phosphorylation and Rac activation induced by this chemokine. Altogether, our studies indicate a novel mechanism by which the Slit/Robo complex may inhibit the CXCR4/CXCL12-mediated chemotaxis of T cells.

Keywords

leukocytes; migration; chemokine; inflammation; signal transduction

INTRODUCTION

The Slit family of genes consists of large extracellular matrix-secreted and membrane-associated glycoproteins [1–3]. The Slits (Slits 1–3) are ligands for the repulsive guidance receptor (Robo) gene family [4–6]. Slit was originally found to be expressed in neurons and glial cells in the neuronal system and was later shown to play the role of a multifunctional signaling molecule by acting as a silencer and a repellent and perhaps as a branching and elongation factor [4,7–12]. Slit consists of a family of three genes (Slit-1, Slit-2, and Slit-3), which have been cloned from different model systems [13–15].

The roundabout (Robo) receptors are molecular targets for Slit [1,6,15,16]. Robo receptors are highly conserved from fruit flies to mammals and constitute a novel subfamily of Ig superfamily proteins [12]. Robo-1 is a single-pass transmembrane receptor whose extracellular

[1] Correspondence: Beth Israel Deaconess Medical Center, Harvard Institutes of Medicine, 4 Blackfan Circle, Room 343, Boston, MA 02115, USA. E-mail: rganju@bidmc.harvard.edu.

region contains five Ig and three fibronectin III repeats. The large intracellular region of Robo-1 contains four conserved motifs designated CC0, CC1, CC2, and CC3 [7,17]. Identification of Robo mutations during genetic screens for guidance defects has revealed the importance of Slit/Robo signaling in axonal guidance and cell migration [16–20].

The intracellular transduction mechanism for Slit/Robo signaling is not well defined. Work in Drosophila indicates that the Abelson kinase (Abl) and the Enabled (Ena) proteins are involved in this process and that they interact with the CC0, CC1, and CC3 domains of Robo-1, respectively [17]. Extracellular application of Slit can increase the intracellular interaction between soluble recombinant GTPase-activating protein 1 (srGAP1) and Robo [12,20]. Slit can also increase the interaction between srGAP1 and Cdc42 but decreases the interaction of Cdc42 with RhoA [12,20].

Until recently, functional studies of the Slit/Robo interactions were confined to the CNS, where the interactions were observed to mediate repulsive cues on axons and growth cones during neural development [1,7,11,15,21,22]. More recently, there have been several reports, which indicate that the expressions of Slit and Robo are widely distributed and that these molecules regulate various biological functions in the body including the immune system [5,6,10,23–33]. For example, the Robo-4 (magic roundabout) receptor was shown to be expressed by endothelial cells. Furthermore, Slit-2 was shown to block the vascular endothelial growth factor (VEGF) and EGF-mediated migration of endothelial cells [34–36], as well as to inhibit the migration of leukocytes, dendritic cells (DC), and breast cancer cells [29–32]. Although Slit has been reported to affect the chemokine-induced migration of different cell types, the mechanism by which the Slit/Robo complex blocks migration has not been elucidated.

The CXCL12/CXCR4 axis plays an important role in immune and inflammatory responses through the regulation of cell migration and growth [37–41]. It is well established that CXCR4 plays a crucial role in the pathogenesis of several diseases including HIV, autoimmune diseases, atherosclerosis, and other inflammatory disorders [37–47]. CXCL12/CXCR4 has also been shown to play an important role in the metastasis of different cancers [44,48]. These results suggest that inhibition of the CXCR4/CXCL12 axis has potential value in the prevention and treatment of various diseases.

In the present study, we observed that Slit-2 inhibits CXCL12-induced chemotaxis as well as the transendothelial migration of T lymphocytes and monocytes. Moreover, our signaling studies revealed that Slit-2 enhances an association between Robo-1 and CXCR4 and down-regulates the activities of several critical downstream signaling molecules. This study provides novel insights into Slit/Robo-mediated, antichemotactic signaling mechanisms.

MATERIALS AND METHODS

Cells, cell culture, and constructs

The human Jurkat T cell line was obtained from American Type Culture Collection (Manassas, VA, USA). The cell lines were cultured at 37°C in 5% CO_2 in RPMI 1640 with 10% FCS, 2 mM glutamine, 50 μg/ml penicillin, and 50 μg/ml streptomycin. 293T cells, generously provided by Hava Avraham (Beth Israel Deaconess Medical Center, Boston, MA, USA), were maintained in DMEM with 10% FBS and 1% penicillin-streptomycin at 37°C in 5% CO_2. Yi Rao (Washington University, St. Louis, MO, USA) generously provided all of the Robo-1 and Slit-2 constructs.

Flow cytometry

To determine Robo-1 receptor expression, Jurkat T cells, PBMCs, and monocytes (1×10^6) were washed twice with PBS, resuspended in 100 μl PBS with 5% FBS and Robo-1 antibodies

(Developmental Studies Hybridoma Bank, University of Iowa, Iowa City, IA, USA) or with mouse IgG antibodies as a control, and then incubated at 4°C. Cells were washed three times in PBS containing 5% FBS and incubated with anti-mouse IgG labeled with FITC for 2 h at 4°C. The cells were next washed three times with ice-cold PBS, 5% FBS buffer, resuspended in 200 μl PBS, and then analyzed by flow cytometry to determine the surface expression levels of the receptor.

Calcium flux assay

Jurkat T cells were washed twice with HBSS (Mediatech Co., Herndon, VA, USA) and resuspended at 1×10^6 cells/ml in HBSS. The cells were pretreated with Slit-2 supernatant (100 μg/ml) and control supernatant (100 μg/ml) for 30 min at 37°C. They were next loaded with Indo-1 AM by adding 5 μl working (1 μg/ml/μl DMSO) Indo-1 AM solution and incubated for 45 min at 37°C. The cells were then treated with CXCL12 (50 ng/ml) and analyzed for calcium mobilization by flow cytometry (FACSVantage, BD Biosciences, San Jose, CA, USA).

Receptor-binding assay

The binding of CXCL12 to its receptor CXCR4 was assessed by using 1 ng/ml ^{125}I-labeled CXCL12 (Amersham Biosciences, Piscataway, NJ, USA) in the presence of various concentrations of purified Slit-2 or unlabeled CXCL12 (PeproTech, Rocky Hill, NJ, USA) [29]. Briefly, Jurkat T cells at 10^7/ml in RPMI 1640 [containing 1% BSA (w/v) and 25 mM/L HEPES] were incubated in the presence of various concentrations of purified Slit-2 or unlabeled CXCL12, together with 1 ng/ml ^{125}I-labeled CXCL12 for 1 h at room temperature and then washed three times with cold RPMI 1640 (containing 25 mM/L HEPES). Cell pellet-associated radioactivity was determined in a γ-counter.

Preparation of PBMCs, monocytes, and CD4$^+$ T cells

Primary mononuclear cells were isolated from heparinized venous blood, as described before [49]. Blood, collected from healthy donors, according to a protocol, which has been approved by the Beth Israel Deaconess Medical Center Committee on Clinical Investigations, was subjected to Ficoll-Paque density gradient centrifugation at 3000 rpm for 25 min. For the primary lymphocyte culture, the cells were suspended in RPMI containing 15% FCS, 2 mM glutamine, 50 IU/ml penicillin, and 50 μg/ml streptomycin. Monocytes were depleted by two rounds of adherence to plastic. Nonadherent cells were stimulated with phytohemagglutinin (5 μg/ml) for 3 days. Cells were then removed and placed in fresh medium supplemented with recombinant human IL-2 (Advanced Biotechnologies, Columbia, MD, USA). The purity of the PBMCs was checked by flow cytometry using CD3 antibody. Two-week-old cells were used for various experiments. For the primary CD4$^+$ T cells, PBMCs were washed with PBS containing 2% BSA, and CD4$^+$ T cells were collected by using the Easy$^{™}$ CD4$^+$ T cell enrichment system (StemCell Technologies, Vancouver, BC, Canada), according to the manufacturer's instructions. Briefly, CD4$^+$ T cells were negatively isolated from a mononuclear cell sample by treatment with a CD8, CD14, CD16, CD19, CD56, TCRγ/δ, Glycophorin A, and Dextran antibody mix. The antibody-coupled cells were depleted by using magnetic Dextran iron particles. The purity was checked by flow cytometry using CD4 antibody. For the primary monocytes, PBMCs were washed with PBS containing 0.1% BSA, and then the monocytes were collected by using the Dynal negative-selection system (Dynal Biotech, Norway), according to the manufacturer's instructions. Briefly, monocytes were negatively isolated from the mononuclear cell sample by treatment with a CD2, CD7, CD16, CD19, CD56, and CD235a antibody mix. This was followed by depletion of the antibody-coupled cells with Dynal beads. The purity of the monocytes was checked by flow cytometry using CD14 antibody.

Preparation of Slit-2 and control supernatant

Slit-2 was obtained from the supernatants of myc-tagged, Slit-2-transfected human embryonic kidney (HEK) cells, according to published procedures [4,30]. Briefly, conditioned medium containing Slit-2/myc proteins was collected from Slit-2/myc-transfected HEK293 cells and concentrated using Amicon Ultra-100K filters. Slit-2 expression was detected with anti-c-myc or anti-Slit-2 antibody. Control preparations obtained from the vector-transfected cell lines were then generated using the same procedures as those used for the Slit-2 preparations. The partially purified Slit-2 was enriched further on a Superdex 200 gel filtration column using the Pharmacia (Uppsala, Sweden) fast protein liquid chromatography (FPLC) system. The fractions were analyzed on 8% SDS-PAGE gels, stained with Silver stain or on immunoblots, and probed with anti-myc antibodies. The fractions harboring Slit-2 were dialyzed with PBS, concentrated, and used for the chemotaxis assays.

Transfections

The CXCR4, hemagglutinin-tagged, full-length Robo-1 [HA-FL-Robo-1 (R1)] and mutant constructs [HA-Robo-1 ΔCC3 (R1ΔCC3)] were transfected into 293T cells using Lipofectamine transfection reagents, according to the manufacturer's instructions (Invitrogen, Life Technologies, Carlsbad, CA, USA). Briefly, ~4×10^6 cells were plated in six-well, tissue-culture plates and grown to a confluency of 50% after 16 h of incubation at 37°C with transfection medium containing different expression vectors. This was followed by the addition of medium with serum, after which the cells were incubated further for another 36 h. The transfection efficiency was checked by Western blot analysis. For the Jurkat T cell transfection, cells were washed with PBS and resuspended in Nucleofector V solution at 5×10^6 cells/100 μl. Different plasmids (2 μg) were mixed with the cellular suspensions, transferred to a 2.0-mm electroporation cuvet, and nucleofected (Program No. S-018) using the Amaxa Nucleofector™ device (Amaxa Biosystems, Cologne, Germany). Following transfection, the cells were transferred immediately to complete medium and cultured at 37°C for 36 h. Transfection efficiency was monitored by using the pmaxGFP plasmid as a control and by Western blotting procedures.

Small interfering RNA (siRNA)-mediated knockdown

siRNA-mediated knockdown of Robo-1 was performed using ON-TARGET-plus SMARTpool Robo-1 siRNA (Dharmacon, Inc., Boulder, CO, USA), according to the manufacturer's protocol. Briefly, Jurkat T cells were electroporated with 250 nM siRNA using the Amaxa system (Amaxa Biosystems), as mentioned above. The respective, nontargeted siRNA SMARTpool was used as a control. Robo-1 siRNA-mediated knockdown was estimated by detecting Robo-1 receptor expression 48 h after the initial transfection by using flow cytometry.

Cell viability assay

Jurkat T cells were washed twice with RPMI 1640 and suspended in the RPMI-1640 medium at a concentration of 1×10^6 cells/ml. Cell suspension (100 μl/well) was loaded into 96-well plates and treated with Slit-2 supernatant (100 μg/ml) or control supernatant (100 μg/ml) for various time-points. The number of viable cells was quantified by using the CellTiter 96® Aqueous kit (Promega, Madison, WI, USA), as per the manufacturer's instructions.

Stimulation of cells

The cells were stimulated as described earlier [50]. Briefly, Jurkat T cells were washed twice with 1× HBSS (Mediatech Co.), suspended at 10×10^6 cells/ml in the same solution, and starved for 1 h at 37°C in 5% CO_2. The cells were pretreated with Slit-2 supernatant and control supernatant (100 μg/ml), followed by stimulation with 100 ng/ml CXCL12. After stimulation,

the cells were microfuged for 10 s and lysed with modified radioimmune precipitation assay buffer [50 mM Tris-HCl, pH 7.4, 1% Nonidet P-40 (NP-40), 150 mM NaCl, 0.5% sodium deoxycholate, 200 mM PMSF, 10 μg/ml aprotinin, 1 μg/ml each leupeptin and pepstatin, 2 mM each sodium vanadate and sodium fluoride, and 0.25 M sodium pyrophosphate]. Total cell lysates were clarified by centrifugation at 10,000 *g* for 10 min. Protein concentrations were determined by a Bio-Rad (Hercules, CA, USA) protein assay kit. The cell lysates were used for the immunoprecipitation, immunoblotting, and kinase assays.

Immunoprecipitation

Immunoprecipitation analysis was done as described [50]. Briefly, equivalent amounts of protein from each sample were precleared by incubation with protein-A-Sepharose CL-4B or protein G-Sepharose (Amersham Biosciences) for 1 h at 4°C. The supernatant from each sample was collected after brief centrifugation. A different primary antibody was added for each experiment, and the samples were incubated at 4°C for 4 h. The immune complexes were precipitated with 50 μl protein-A-Sepharose CL-4B (50% suspension) or protein-G-Sepharose (10% suspension) overnight at 4°C or for 36 h for the anti-CXCR4 immunoprecipitations. The nonspecific, bound proteins were removed by washing the Sepharose beads three times with modified radioimmune precipitation assay buffer and once with 1× PBS. The immune complexes bound to the beads were subjected to kinase assay or solubilized in 40 μl 2× Laemmli buffer and analyzed further by Western blotting, as described below.

Western blotting

Western blot analyses were done as described previously [50]. Briefly, equivalent amounts of protein from each sample were run on 8% SDS-PAGE gels and transferred to nitrocellulose membranes, which were blocked with 5% nonfat dry milk and incubated with primary antibody for 2 h at room temperature or overnight at 4°C. The blots were washed and incubated with secondary antibody coupled to HRP for 2 h at room temperature or overnight at 4°C. The bands were visualized by using the ECL system (Amersham Biosciences). The data are representative of findings from three experiments.

Chemotaxis and transendothelial migration assays

Assays were done as described previously [50,51]. Briefly, Jurkat T cells were washed twice, and 2.5×10^6 cells/ml were suspended in medium containing RPMI 1640 with 2.5% BSA. The chemotaxis assay was performed in 24-well plates containing 5 μm porosity inserts (Co-Star Corp., Kennebunk, ME, USA). Cells were pretreated with Slit-2 supernatant and control supernatant (100 μg/ml) for 30 min at 37°C. Each cell preparation (100 μL) was loaded onto the upper well, and then 0.6 ml medium containing chemokine (CXCL12) and the Slit-2 supernatant or control supernatant (100 μg/ml) was added to the lower chamber. The plates were incubated for 3 h at 37°C in 5% CO_2. After incubation, the inserts were removed carefully, and the viable cells were counted using standard procedures. For the transendothelial migration assay, endothelial cells were cultured on the upper side of the membrane for 2 days before the start of the experiment and then left unstimulated. The integrity of the confluent HUVEC monolayer was assessed by microscopic observation. The results are expressed as the number of cells migrating to the bottom chamber. Each experiment was performed three or four times in triplicate.

Cell adhesion assays

The T cell adhesion assay was performed by using the Vybrant™ cell adhesion assay kit (Molecular Probes, Eugene, OR, USA). Briefly, Jurkat T cells were washed twice with PBS and resuspended in RPMI 1640 at 5×10^6 cells/ml. Cells were then treated with 5 μM Calcein AM at 37°C for 30 min. The cells were washed twice with prewarmed RPMI 1640, loaded on

microplate wells containing confluent HUVEC (medium removed), and then incubated at 37° C for 60 min. Nonadherent, Calcein-labeled cells were removed by careful washing with prewarmed RPMI 1640, and 200 μl PBS was added to each well. Fluorescence was measured at an absorbance maximum of 494 nm and emission maximum of 517 nm. Data were analyzed by taking the control as 100% adhesion.

GST pull-down assay

The cytoplasmic domain and mutant cytoplasmic domain (ΔCC3) of Robo-1 were cloned into *Eco*RI-*Sal*I sites of the pGEX-6P-2 vector. The GST-FL-Robo-1 cytoplasmic domain (GST-cytR1) and GST-Robo-1 mutant cytoplasmic domain (GST-cytR1-ΔCC3) vectors were then transfected into *Escherichia coli* (BL12pLys) cells and expressed on induction with 1 mM isopropyl-β-D-thiogalactoside for 3 h at 30°C. The bacteria-expressing fusion proteins were lysed by sonication in TBS and their expression confirmed by SDS-PAGE gels followed by Coomassie blue staining. The fusion proteins were then purified by glutathione Sepharose 4B beads (Amersham Pharmacia, UK). For the pull-down assay, Jurkat T cells were stimulated with Slit-2 (100 μg/ml) for 30 min at 37°C. The cells were lysed, and cell lysates were incubated with 100 μl immobilized glutathione resin (50% slurry) for 30 min at 4°C. After washing, purified GST-fusion proteins or GST protein (50 μg) were added to the lysates. The binding was performed at 4°C for 3 h. Next, 100 μl immobilized glutathione resin (50% slurry) was added to the lysates, which were then incubated for 1 h at 4°C. The resin was washed four times with 500 μl TBS buffer containing 0.5% NP-40 and 1 mM DTT. Proteins were eluted in 50 μl SDS sample buffer and analyzed by 4–12% SDS-PAGE (Invitrogen, Life Technologies).

Kinase assay

Kinase assays for Src, Lck, and Lyn were done as described [50,52]. Briefly, the immune complexes obtained by immunoprecipitating the cell lysates with antibodies to Src, Lck, and Lyn were washed twice with radioimmune precipitation assay buffer and twice with kinase buffer (20 mM HEPES, pH 7.4, 50 mM NaCl, 10 μM Na_3VO_4, 5 mM $MgCl_2$, 5 mM $MnCl_2$). Last, the immune complexes were incubated in a total volume of 25 μl kinase buffer containing a final concentration of enolase (10 μg/ml) as a substrate, 10 μM ATP, and 5 μCi [γ-^{32}P]ATP (specific activity: 3000 Ci/mmol) for 30 min at 30°C. The proteins were separated on 12% SDS-PAGE, and the bands were detected by autoradiography. Quantitative analysis of protein phosphorylation was done by measuring band density using the Alpha ImageTech Imaging system.

JNK and p38 MAPK assays

The JNK and p38 MAPK assays were performed as described earlier [51]. Briefly, cell lysates were immunoprecipitated with JNK antibody (Santa Cruz Biotechnology, Santa Cruz, CA, USA). The immune complexes were washed twice with radioimmunoprecipitation assay (RIPA) buffer and once in kinase wash buffer (20 mM HEPES, pH 7.5, 2.5 mM $MgCl_2$, 50 mM NaCl, 0.1 mM EDTA, 0.05% NP-40) and resuspended in JNK-kinase buffer (20 mM HEPES, pH 7.7, 10 mM $MgCl_2$, 2 mM DTT, 20 mM β-glycerophosphate, 20 mM p-nitrophenylphosphate, 0.1 mM Na_3VO_4, 20 μM ATP) containing 5 μCi [γ-^{32}P] ATP (specific activity: 3000 Ci/mmol) and 10 μg myelin basic protein (MBP; Upstate Biotechnology, Lake Placid, NY, USA). The kinase reaction was carried out for 20 min at 37°C. The reaction was terminated by adding 2× SDS sample buffer and boiling the samples for 5 min. Proteins were separated on 12% SDS-PAGE gel and detected by autoradiography. For the p38 MAPK assay, cell lysates were immunoprecipitated with p38 MAPK antibody (Santa Cruz Biotechnology). The immunocomplexes were washed twice with RIPA buffer and once in JNK-kinase buffer and then incubated in JNK-kinase buffer containing 7 μg MBP (Upstate Biotechnology) and 5 μCi [γ-^{32}P] ATP (specific activity: 3000 Ci/mmol) for 20 min at 30°C. The reaction was

terminated by adding 2× SDS sample buffer and boiling the samples for 5 min. The proteins were separated on 15% SDS-PAGE gel and detected by autoradiography. Quantitative analysis of protein phosphorylation was done by measuring band density using the Alpha ImageTech Imaging system.

Rac activation assay

Rac activation was determined by using the Rac/Cdc42 activation assay kit (SGT445, Upstate Biotechnology) [53]. In brief, cell lysates were incubated with 15 μg/ml p21-activated kinase (PAK)-1 agarose for 60 min at 4°C, according to the protocols of Upstate Biotechnology. Agarose beads were collected by centrifugation, followed by denaturation, boiling of the samples, and SDS-PAGE analysis. Proteins were transferred to nitrocellulose membranes, and Western blotting was performed by using murine anti-human Rac antibody.

Statistical analysis

The results are expressed as the mean ± SD of data obtained from three or four experiments performed in duplicate or triplicate. The statistical significance was determined by the Student's *t*-test.

RESULTS

Expression of Robo receptors in Jurkat T cells, PBMCs, and monocytes

Slit mediates its effect by binding to Robo receptors, which are highly conserved from fruit flies to mammals [4–6]. In mammals, four Robo genes (Robo-1, Robo-2, Robo-3, and Robo-4) have been identified. The extracellular domain of Robo-1 contains five Ig domains and three fibronectin Type III repeats, whereas the intracellular region contains identifiable, conserved motifs designated CC0, CC1, CC2, and CC3. Robo-2 and Robo-3 lack the CC2 and CC3 domains [7,17]. We analyzed the expression of Robo-1 in Jurkat T cells, PBMCs, and monocytes by staining the cells with Robo-1-specific antibody, followed by flow cytometric analysis. As shown, PBMCs (Fig. 1A) and Jurkat T cells (Fig. 1B) exhibited high expression of the Robo-1 receptor, whereas monocytes (Fig. 1C) expressed a moderate amount of Robo-1 receptor.

Slit-2 inhibits the CXCL12-induced chemotaxis, transendothelial migration, and adhesion of T cells

As CXCL12 has been shown to be a potent chemoattractant for various cells of the immune system [37–40], we analyzed whether Slit-2-mediated activation of the Robo-1 receptor could modulate CXCL12-induced T cell chemotaxis. Jurkat T cells and PBMCs were preincubated with Slit-2 supernatant and control supernatant (10 or 100 μg/ml) and then analyzed for chemotaxis toward CXCL12. As shown, the chemotactic response of Jurkat T cells (Fig. 2A) and PBMCs (Fig. 2B) was inhibited significantly in the presence of the Slit-2 supernatant as compared with the control supernatant. Moreover, Slit-2 inhibited the CXCL12-induced chemotaxis in a dose-dependent manner, with a maximum inhibition of ~70%. Slit-2 supernatant was also able to block CXCL12-induced transen-dothelial migration in Jurkat T cells (Fig. 2C) and PBMCs (Fig. 2D). We then studied the effect of Slit-2 on the CXCL12-induced adhesion of Jurkat T cells to endothelial cells. As shown in Figure 2E, pretreatment with Slit-2 supernatant significantly inhibited the CXCL12-mediated adhesion of Jurkat T cells to endothelial cells.

To confirm that Slit-2 inhibits CXCL12-induced chemotaxis, Slit-2 was immunodepleted (I.D.) from the concentrated supernatants using anti-myc antibody, and then the I.D. supernatants were analyzed for their inhibitory activities. We found that the I.D. supernatants were not able

to inhibit the chemotaxis of Jurkat T cells in response to CXCL12 (Fig. 3A). We next determined the antichemotactic activity of highly purified Slit-2, which was purified using the Superdex 200 FPLC system. The purity of the sample was determined by Silver staining and immunoblotting (Fig. 3C). Purified Slit-2 was able to block the CXCL12-induced chemotaxis in a dose-dependent manner, and a maximum inhibition (~55%) was obtained at 500 ng/ml (2.6 nM) of Slit-2 (Fig. 3B).

To confirm that the Slit-2/Robo-1 interaction mediates the inhibition of CXCL12-induced chemotaxis, we used siRNA-driven knockdown of Robo-1 in Jurkat T cells and studied the effect of Slit-2 on CXCL12-induced chemotaxis. As shown in Figure 3D, 65–70% knockdown of Robo-1 was observed in the Jurkat T cells transfected with the Robo-1 siRNA, as compared with cells transfected with the control (nontargeted) siRNA. Furthermore, Robo-1 knocked-down cells did not show any significant Slit-2-mediated inhibition of the CXCL12-induced chemotaxis (Fig. 3E).

Slit-2 inhibits the CXCL12-induced chemotaxis of primary monocytes and $CD4^+$ T cells

We isolated monocyte and $CD4^+$ T cell populations by negative selection. The purity of the monocytes (80–85%) and $CD4^+$ T cells (>90%) was analyzed by using a flow cytometer. We also used flow cytometry to analyze Robo-1 expression in these cell populations and found that ~60% of the monocytes and ~48% of the $CD4^+$ T cells showed Robo-1 expression (data not shown). We then analyzed the effect of Slit-2 on the CXCL12-induced chemotaxis of monocytes and $CD4^+$ T cells. As shown, the chemotactic response of the Slit-2 supernatant-pretreated monocytes (Fig. 4A) and $CD4^+$ T cells (Fig. 4B) was significantly inhibited toward CXCL12 as compared with the control supernatant-pretreated cells.

Slit-2 induces an association between Robo-1 and CXCR4

We then analyzed the possible molecular mechanisms involved in the Slit-2-mediated inhibition of chemotaxis induced by CXCL12. Initially, we evaluated the cytotoxic effects in Slit-2-stimulated cells. As shown in Figure 5A, Slit-2-treated Jurkat T cells did not show any cytotoxicity. Next, we studied the effect of Slit-2 on CXCL12-induced calcium flux in Jurkat T cells. We found no significant change in the CXCL12-induced calcium flux in Jurkat T cells pretreated with Slit-2 supernatant or control supernatant (Fig. 5B). This result indicates that Slit-2/Robo-1 did not induce heterologous desensitization of CXCR4. Moreover, we did not find any significant change in ^{125}I-CXCL12 binding to CXCR4 in Jurkat T cells in the presence of different concentrations of Slit-2 supernatant (Fig. 5C). However, unlabeled CXCL12 (100 ng/ml), which was used as a control, did inhibit the ^{125}I-CXCL12 binding to CXCR4 (Fig. 5C). These results suggest that Slit-2 does not inhibit the binding affinity of CXCL12 to its receptor. We also studied the association between Robo-1 and CXCR4. To analyze their interaction, we overexpressed HA-FL-Robo-1 and FLAG-tagged CXCR4 (CXCR4) plasmids in 293T cells and then stimulated the cells with Slit-2 supernatant or control supernatant preparation. As shown in Figure 6A, Robo-1 associated with CXCR4 and the Slit-2 supernatant enhanced this association when compared with the control supernatant-treated cells. We also confirmed this enhanced association of the two receptors following Slit-2 treatment of the Robo-1 overexpressing Jurkat T cells by using coimmunoprecipitation techniques (Fig. 6B).

The CC3 domain of the Robo-1 intracellular region plays an important role in the Robo-1/CXCR4 coassociation and in the Slit-2-mediated inhibition of Jurkat T cell chemotaxis induced by CXCL12

To further analyze the role of Robo-1 in the Slit-2-mediated inhibition of chemotaxis induced by CXCL12, we overexpressed HA-FL-Robo-1 (R1; Fig. 7A), an HA-tagged mutant form of Robo-1 (Robo-1 with a deletion in the CC3 motif, HA-Robo-1 ΔCC3; R1ΔCC3; Fig. 7A) and FLAG-tagged CXCR4 in the 293T cells. We then treated the cells with Slit-2 supernatant and

determined the coassociation of Robo-1 and CXCR4 by immunoprecipitation assays. We observed reduced coassociation of Robo-1 with CXCR4 in cells which overexpressed the mutant Robo-1 receptor lacking the CC3 motif (HA-Robo-1 ΔCC3; Fig. 7B). In addition, we confirmed these results by using a GST pull-down assay. As shown in Figure 7C, an interaction between the fused GST-cytR1 and CXCR4 was observed, whereas no such interaction was observed in samples containing GST alone. In contrast, the fused GST-cytR1 ΔCC3 showed a significantly reduced interaction with CXCR4. This suggests that the CC3 domain of the Robo-1 intracellular region may regulate the association between Robo-1 and CXCR4. We further analyzed the functional significance of the CC3 domain of Robo-1 in regulating CXCL12-induced chemotaxis. We performed chemotaxis assays in mutant Robo-1 (HA-Robo-1 ΔCC3)-overexpressing Jurkat T cells and observed no significant inhibition of CXCL12-induced chemotaxis by Slit-2 in the cells which overexpressed the Robo-1 receptor lacking the CC3 domain. However, a signifi-cant inhibition of chemotaxis was observed in the presence of Slit-2 in Jurkat T cells overexpressing HA-FL-Robo-1 (Fig. 7D). The transfection efficiency of each construct was analyzed by Western blotting. As shown in Figure 7E, a high transfec-tion efficiency for both of the constructs was observed in the Jurkat T cells. This result suggests that the CC3 domain of the Robo-1 receptor is important for the Slit-2-mediated inhibition of chemotaxis induced by CXCL12.

Effect of Slit-2 on Src and MAPK activities

Src kinases are early signaling molecules activated in the CXCL12/CXCR4 pathway [54–56]. These kinases have been shown to associate with focal adhesion kinases and to play a crucial role in the signal transduction implicated in cellular migration and adhesion [57,58]. Src kinases have also been shown to regulate the phosphorylation and activation of various signaling molecules, including components of focal adhesion complexes [54–57]. We thus studied the effect of Slit-2 on the CXCL12-induced activation of Src kinases in Jurkat T cells. As shown in Figure 8, we observed significant inhibition of Src kinase and Lck kinase activities in the Slit-2 supernatant-pretreated cells when compared with the control supernatant-pretreated cells. However, no significant change in Lyn kinase and MAPK activities was observed between the Slit-2 supernatant-pretreated and control supernatant-pretreated cells (Fig. 8, A–C).

Slit-2 inhibits the CXCL12-induced phosphorylation of Akt as well as Rac activation

The PI-3K pathway is reported to play an important role in CXCL12-induced migration [54–57]. In addition, PI-3K has been shown to activate Akt, and CXCL12 has been found to enhance Akt phosphorylation [59]. Hence, we analyzed the effect of Slit-2 on the CXCL12-induced phosphorylation of Akt in Jurkat T cells. As shown in Figure 8D, the Slit-2 supernatant significantly blocked the CXCL12-induced phosphorylation of Akt when compared with the control supernatant. In addition, Slit-2 alone inhibited the basal level of Akt activity. Equal amounts of Akt protein were present in each lane (Fig. 8D, lower panel).

Rac, a member of the Rho-GTPase family, plays an important role in regulating cytoskeletal dynamics during the chemotaxis of various cell types. In addition, CXCL12 has been shown to activate Rac, and crosstalk between activated Rac and the PI-3K pathway has been reported during immune cell migration [60–62]. Thus, we studied the effect of Slit-2 on Rac activation and observed that the Rac activation induced by CXCL12 was also inhibited significantly in the Slit-2-treated cells as compared with control-treated cells (Fig. 8E).

DISCUSSION

The chemokine-induced transendothelial migration and chemotaxis of immune cells play an important role in inflammation and autoimmune disorders [42–46,48]. Recently, an

endogenous factor termed Slit was shown to inhibit the migration of leukocytes and DC [30, 32]. Slit, which binds to the Robo receptor, has been shown previously to play a role as a multi-factorial molecule in the nervous system by acting as a silencer, repellent, and branching and elongation factor [4,7–12]. In this study, we demonstrate that Slit-2 can inhibit CXCL12-induced and CXCR4-mediated T cell and monocyte chemotaxis. Slit-2 also blocked T cell transendothelial migration, which is an important step in inflammation. It has been well established that the CXCL12/CXCR4 axis modulates the pathogenesis of various inflammatory disorders, such as autoimmune diseases and atherosclerosis [42–46,48]. It has also been shown that the CXCL12/CXCR4 axis plays a pivotal role in the retention/homing of hematopoietic stem cells into the bone marrow microenvironment and more recently, that the perturbation of this axis is essential for the egress of hematopoietic stem/progenitor cells from the bone marrow into the peripheral blood [44]. These studies suggest that use of Slit-2 to block CXCR4/CXCL12-induced chemotactic responses has therapeutic potential for various disorders.

Although Slit-2 has been shown to inhibit the CXCL12-induced migration of different cell types [29,30,32–36], the molecular mechanism of the Slit-2-mediated inhibition of chemotaxis is not well known. In this regard, we observed an enhanced association between the CXCR4 and Robo-1 receptors upon stimulation with Slit-2 in T cells. The functional interactions of Robo with other receptors have also been observed during midline crossing-over of axonal growth cones in the nervous system [6]. Slit-induced activation of the Robo receptor silences the attractive effects of netrin-1 through direct binding of the cytoplasmic domain of Robo to that of the netrin receptor deleted in colorectal cancer (DCC) [6]. This interaction of the cytoplasmic tails of the two receptors is mediated by short, conserved domains in each receptor (CC1 in Robo and P3 in DCC) [6]. In the present study, we demonstrate that the CC3 domain of the cytoplasmic region of Robo-1 plays an important role in its interaction with CXCR4 and in the inhibition of chemotaxis. These studies indicate functional crosstalk between two distinct families of guidance molecules, one working through single transmembrane receptors and the other through seven-transmembrane G protein-coupled receptors.

The intracellular signaling mechanism in the Slit/Robo pathway is not well defined. Work in Drosophila indicates that the Abl and the Ena proteins are involved in Slit/Robo signaling [17]. Moreover, Slit enhances the association between srGAP1 and Robo via the CC3 motif, and this localization may induce the inactivation of Cdc42 [12,20].

Thus, we further analyzed Slit/Robo-mediated, antichemotactic signaling mechanisms in T cells and observed that Slit-2 inhibited CXCL12-induced Src kinase activity in these cells. c-Src has been shown previously to play an important role in the phosphorylation of components of focal adhesion complexes [52,54–56]. We also found that Slit-2 blocked Lck kinase activity, which is reported to be a key regulator of T cell migration [55], although we did not observe any change in Lyn kinase activity. The direct involvement of Lck kinase in CXCL12-induced T cell chemotaxis has been demonstrated in the Lck-deficient, Jurkat-derived cell line JCaM1.6 [55].

In our study, we also investigated the effect of Slit-2 on the downstream pathways, which are known to mediate transcriptional activation. Earlier we had shown that CXCL12 enhances Akt phosphorylation [49]. Activation of the PI-3K/Akt pathway by CXCL12 is known to regulate the chemotaxis of various cell types [49,59]. We observed here that Slit-2 inhibited the CXCL12-induced phosphorylation of Akt. However, Slit-2 had no effect on the CXCL12-induced activation of MAPK in T cells. It is interesting that Slit-2 has been shown to inhibit the CXCL12-induced phosphorylation of Erk1/2 in breast cancer cells [29]. It is further known that MAPK does not regulate the CXCL12-induced chemotaxis of T cells [49]. In addition, we observed that Slit-2 inhibited the activation of Rac, which has been shown previously to participate in the chemokine-induced migration of macrophages [61]. Moreover, in neuronal

cells, it has been observed that the Slit/Robo pathway inhibits the activity of Cdc42 (a member of the Rho-GTPase family) by inducing an interaction between the intracellular domain of Robo and the Rho-GAPs [20]. Altogether, Slit-2-induced/Robo-1-mediated signaling results in decreased activation of various downstream signaling molecules of the CXCR4 pathway, which might inhibit the CXCL12-induced activation of focal adhesion components and downstream effector molecules.

Our data imply an important role for Slit-2 in CXCL12-induced chemotaxis/chemoinvasion. Specifically, our results suggest that Slit-2 regulates chemotaxis by a novel mechanism involving the interaction of Robo-1 with CXCR4 as well as by down-modulating the activities of focal adhesion complex components and the PI-3K/Akt pathway. These studies add a new dimension to our understanding of CXCR4-mediated chemotaxis and may yield new, therapeutic interventions for autoimmune, inflammatory, and other diseases.

Acknowledgements

The research is supported in part by grants from the National Institutes of Health AI49140 and A109527, Susan G. Komen Breast Cancer Foundation, and Department of Defense award #W81XWH-05-1-0465 to R. K. G. We thank Dr. Yi Rao (Washington University School of Medicine, St. Louis, MO, USA) for generously providing the Slit-2 and Robo-1 constructs.

References

1. Brose K, Bland KS, Wang KH, Arnott D, Henzel W, Goodman CS, Tessier-Lavigne M, Kidd T. Slit proteins bind Robo receptors and have an evolutionarily conserved role in repulsive axon guidance. Cell 1999;96:795–806. [PubMed: 10102268]
2. Kidd T, Bland KS, Goodman CS. Slit is the midline repellent for the Robo receptor in Drosophila. Cell 1999;96:785–794. [PubMed: 10102267]
3. Chen JH, Wu W, Li HS, Fagaly T, Zhou L, Wu JY, Rao Y. Embryonic expression and extracellular secretion of Xenopus slit. Neuroscience 2000;96:231–236. [PubMed: 10683427]
4. Li HS, Chen JH, Wu W, Fagaly T, Zhou L, Yuan W, Dupuis S, Jiang ZH, Nash W, Gick C, Ornitz DM, Wu JY, Rao Y. Vertebrate slit, a secreted ligand for the transmembrane protein roundabout, is a repellent for olfactory bulb axons. Cell 1999;96:807–818. [PubMed: 10102269]
5. Piper M, Georgas K, Yamada T, Little M. Expression of the vertebrate Slit gene family and their putative receptors, the Robo genes, in the developing murine kidney. Mech Dev 2000;94:213–217. [PubMed: 10842075]
6. Stein E, Tessier-Lavigne M. Hierarchical organization of guidance receptors: silencing of netrin attraction by slit through a Robo/DCC receptor complex. Science 2001;291:1928–1938. [PubMed: 11239147]
7. Wong K, Park HT, Wu JY, Rao Y. Slit proteins: molecular guidance cues for cells ranging from neurons to leukocytes. Curr Opin Genet Dev 2002;12:583–591. [PubMed: 12200164]
8. Bashaw GJ, Goodman CS. Chimeric axon guidance receptors: the cytoplasmic domains of slit and netrin receptors specify attraction versus repulsion. Cell 1999;97:917–926. [PubMed: 10399919]
9. Wu W, Wong K, Chen J, Jiang Z, Dupuis S, Wu JY, Rao Y. Directional guidance of neuronal migration in the olfactory system by the protein Slit. Nature 1999;400:331–336. [PubMed: 10432110]
10. Fernandis AZ, Ganju RK. Slit: a roadblock for chemotaxis. Sci STKE 2001 2001:PE1.
11. Chen JH, Wen L, Dupuis S, Wu JY, Rao Y. The N-terminal leucine-rich regions in Slit are sufficient to repel olfactory bulb axons and subventricular zone neurons. J Neurosci 2001;21:1548–1556. [PubMed: 11222645]
12. Ghose A, Van Vactor D. GAPs in Slit-Robo signaling. Bioessays 2002;24:401–404. [PubMed: 12001262]
13. Holmes GP, Negus K, Burridge L, Raman S, Algar E, Yamada T, Little MH. Distinct but overlapping expression patterns of two vertebrate slit homologs implies functional roles in CNS development and organogenesis. Mech Dev 1998;79:57–72. [PubMed: 10349621]

14. Itoh A, Miyabayashi T, Ohno M, Sakano S. Cloning and expressions of three mammalian homologues of Drosophila slit suggest possible roles for Slit in the formation and maintenance of the nervous system. Brain Res Mol Brain Res 1998;62:175–186. [PubMed: 9813312]
15. Yuan W, Zhou L, Chen JH, Wu JY, Rao Y, Ornitz DM. The mouse SLIT family: secreted ligands for ROBO expressed in patterns that suggest a role in morphogenesis and axon guidance. Dev Biol 1999;212:290–306. [PubMed: 10433822]
16. Kidd T, Brose K, Mitchell KJ, Fetter RD, Tessier-Lavigne M, Goodman CS, Tear G. Roundabout controls axon crossing of the CNS midline and defines a novel subfamily of evolutionarily conserved guidance receptors. Cell 1998;92:205–215. [PubMed: 9458045]
17. Bashaw GJ, Kidd T, Murray D, Pawson T, Goodman CS. Repulsive axon guidance: Abelson and Enabled play opposing roles downstream of the roundabout receptor. Cell 2000;101:703–715. [PubMed: 10892742]
18. Seeger M, Tear G, Ferres-Marco D, Goodman CS. Mutations affecting growth cone guidance in Drosophila: genes necessary for guidance toward or away from the midline. Neuron 1993;10:409–426. [PubMed: 8461134]
19. Rhee J, Mahfooz NS, Arregui C, Lilien J, Balsamo J, VanBerkum MF. Activation of the repulsive receptor Roundabout inhibits N-cadherin-mediated cell adhesion. Nat Cell Biol 2002;4:798–805. [PubMed: 12360290]
20. Wong K, Ren XR, Huang YZ, Xie Y, Liu G, Saito S, Tang H, Wen L, Brady-Kalnay SM, Mei L, Wu JY, Xiong WC, Rao Y. Signal transduction in neuronal migration: roles of GTPase activating proteins and the small GTPase Cdc42 in the Slit-Robo pathway. Cell 2001;107:209–221. [PubMed: 11672528]
21. Dickson BJ, Senti KA. Axon guidance: growth cones make an unexpected turn. Curr Biol 2002;12:R218–R220. [PubMed: 11909551]
22. Guthrie S. Axon guidance: starting and stopping with slit. Curr Biol 1999;9:R432–R435. [PubMed: 10375520]
23. Greenberg JM, Thompson FY, Brooks SK, Shannon JM, Akeson AL. Slit and robo expression in the developing mouse lung. Dev Dyn 2004;230:350–360. [PubMed: 15162513]
24. Xian J, Clark KJ, Fordham R, Pannell R, Rabbitts TH, Rabbitts PH. Inadequate lung development and bronchial hyperplasia in mice with a targeted deletion in the Dutt1/Robo1 gene. Proc Natl Acad Sci USA 2001;98:15062–15066. [PubMed: 11734623]
25. Anselmo MA, Dalvin S, Prodhan P, Komatsuzaki K, Aidlen JT, Schnitzer JJ, Wu JY, Kinane TB. Slit and Robo: expression patterns in lung development. Gene Expr Patterns 2003;3:13–19. [PubMed: 12609596]
26. Latil A, Chene L, Cochant-Priollet B, Manguin P, Fournier G, Berthon P, Cussenot O. Quantification of expression of netrins, slits and their receptors in human prostate tumors. Int J Cancer 2003;103:306–315. [PubMed: 12471613]
27. Dallol A, Krex D, Hesson L, Eng C, Maher ER, Latif F. Frequent epigenetic inactivation of the SLIT2 gene in gliomas. Oncogene 2003;22:4611–4616. [PubMed: 12881718]
28. Dickinson RE, Dallol A, Bieche I, Krex D, Morton D, Maher ER, Latif F. Epigenetic inactivation of SLIT3 and SLIT1 genes in human cancers. Br J Cancer 2004;91:2071–2078. [PubMed: 15534609]
29. Prasad A, Fernandis AZ, Rao Y, Ganju RK. Slit protein-mediated inhibition of CXCR4-induced chemotactic and chemoinvasive signaling pathways in breast cancer cells. J Biol Chem 2004;279:9115–9124. [PubMed: 14645233]
30. Wu JY, Feng L, Park HT, Havlioglu N, Wen L, Tang H, Bacon KB, Jiang Zh, Xhang Xc, Rao Y. The neuronal repellent Slit inhibits leukocyte chemotaxis induced by chemotactic factors. Nature 2001;410:948–952. [PubMed: 11309622]
31. Havlioglu N, Yuan L, Tang H, Wu JY. Slit proteins, potential endogenous modulators of inflammation. J Neurovirol 2002;8:486–495. [PubMed: 12476344]
32. Guan H, Zu G, Xie Y, Tang H, Johnson M, Xhu X, Kevil C, Xiong WC, Elmets C, Rao Y, Wu JY, Xu H. Neuronal repellent Slit2 inhibits dendritic cell migration and the development of immune responses. J Immunol 2003;171:6519–6526. [PubMed: 14662852]

33. Kanellis J, Garcia GE, Li P, Parra G, Wilson CB, Rao Y, Han S, Smith CW, Johnson RJ, Wu JY, Feng L. Modulation of inflammation by slit protein in vivo in experimental crescentic glomerulonephritis. Am J Pathol 2004;165:341–352. [PubMed: 15215188]
34. Park KW, Morrison CM, Sorensen LK, Jones CA, Rao Y, Chein CB, Wu JY, Urness LD, Li DY. Robo4 is a vascular-specific receptor that inhibits endothelial migration. Dev Biol 2003;261:251–267. [PubMed: 12941633]
35. Wang B, Xiao Y, Ding BB, Zhang N, Yuan X, Gui L, Qian KX, Duan S, Chen Z, Rao Y, Geng JG. Induction of tumor angiogenesis by Slit-Robo signaling and inhibition of cancer growth by blocking Robo activity. Cancer Cell 2003;4:19–29. [PubMed: 12892710]
36. Seth P, Lin Y, Hanai J, Shivalingappa V, Duyao MP, Sukhatme VP. Magic roundabout, a tumor endothelial marker: expression and signaling. Biochem Biophys Res Commun 2005;332:533–541. [PubMed: 15894287]
37. Nagasawa T, Hirota S, Tachibana K, Takakura N, Nishikawa N, Kitamura Y, Yoshida N, Kikutani H, Kishimoto T. Defects of B-cell lymphopoiesis and bone-marrow myelopoiesis in mice lacking the CXC chemokine PBSF/SDF-1. Nature 1996;382:635–638. [PubMed: 8757135]
38. Ma Q, Jones D, Borghesani PR, Segal RA, Nagasawa T, Kishimoto T, Bronson RT, Springer TA. Impaired B-lymphopoiesis, myelopoiesis, and derailed cerebellar neuron migration in CXCR4-and SDF-1-deficient mice. Proc Natl Acad Sci USA 1998;95:9448–9453. [PubMed: 9689100]
39. Zou YR, Kottmann AH, Kuroda M, Taniuchi I, Littman DR. Function of the chemokine receptor CXCR4 in haematopoiesis and in cerebellar development. Nature 1998;393:595–599. [PubMed: 9634238]
40. Petit I, Szyper-Kravitz M, Nagler A, Lahav M, Peled A, Habler L, Ponomaryov T, Taichman RS, Arenzana-Seisdedos F, Fujii N, Sandbank J, Zipori D, Lapidot T. G-CSF induces stem cell mobilization by decreasing bone marrow SDF-1 and up-regulating CXCR4. Nat Immunol 2002;3:687–694. [PubMed: 12068293]
41. Gonzalo JA, Lloyd CM, Peled A, Delaney T, Coyle AJ, Gutierrez-Ramos JC. Critical involvement of the chemotactic axis CXCR4/stromal cell-derived factor-1 α in the inflammatory component of allergic airway disease. J Immunol 2000;165:499–508. [PubMed: 10861089]
42. Moore JP, Kitchen SG, Pugach P, Zack JA. The CCR5 and CXCR4 coreceptors—central to understanding the transmission and pathogenesis of human immunodeficiency virus type 1 infection. AIDS Res Hum Retroviruses 2004;20:111–126. [PubMed: 15000703]
43. Murakami T, Yamamoto N. Roles of chemokines and chemokine receptors in HIV-1 infection. Int J Hematol 2000;72:412–417. [PubMed: 11197206]
44. Kucia M, Reca R, Miekus K, Wanzeck J, Wojakowski W, Janowska-Wieczorek A, Ratajczak J, Ratajczak MZ. Trafficking of normal stem cells and metastasis of cancer stem cells involve similar mechanisms: pivotal role of the SDF-1-CXCR4 axis. Stem Cells 2005;23:879–894. [PubMed: 15888687]
45. De Klerck B, Geboes L, Hatse S, Kelchtermans H, Meyvis Y, Vermeire K, Bridger G, Billiau A, Schols D, Matthys P. Pro-inflammatory properties of stromal cell-derived factor-1 (CXCL12) in collagen-induced arthritis. Arthritis Res Ther 2005;7:R1208–R1220. [PubMed: 16277673]
46. Kodali R, Hajjou M, Berman AB, Bansal MB, Zhang S, Pan JJ, Schecter AD. Chemokines induce matrix metalloproteinase-2 through activation of epidermal growth factor receptor in arterial smooth muscle cells. Cardiovasc Res 2006;69:706–715. [PubMed: 16343467]
47. Hogaboam CM, Carpenter KJ, Schuh JM, Proudfoot AA, Bridger G, Buckland KF. The therapeutic potential in targeting CCR5 and CXCR4 receptors in infectious and allergic pulmonary disease. Pharmacol Ther 2005;107:314–328. [PubMed: 16009428]
48. Muller A, Homey B, Soto H, Ge N, Catron D, Buchanan ME, Murphy E, Yuan W, Wagner SN, Barrera JL, Mohar A, Verastequi E, Zlotnik A. Involvement of chemokine receptors in breast cancer metastasis. Nature 2001;410:50–56. [PubMed: 11242036]
49. Cherla RP, Ganju RK. Stromal cell-derived factor 1 α-induced chemotaxis in T cells is mediated by nitric oxide signaling pathways. J Immunol 2001;166:3067–3074. [PubMed: 11207257]
50. Fernandis AZ, Cherla RP, Ganju RK. Differential regulation of CXCR4-mediated T-cell chemotaxis and mitogen-activated protein kinase activation by the membrane tyrosine phosphatase, CD45. J Biol Chem 2003;278:9536–9543. [PubMed: 12519755]

51. Ganju RK, Brubaker SA, Meyer J, Dutt P, Yang Y, Qin S, Newman W, Groopman JE. The α-chemokine, stromal cell-derived factor-1α, binds to the transmembrane G-protein-coupled CXCR-4 receptor and activates multiple signal transduction pathways. J Biol Chem 1998;273:23169–23175. [PubMed: 9722546]
52. Munshi N, Ganju RK, Avraham S, Mesri EA, Groopman JE. Kaposi's sarcoma-associated herpesvirus-encoded G protein-coupled receptor activation of c-jun amino-terminal kinase/stress-activated protein kinase and lyn kinase is mediated by related adhesion focal tyrosine kinase/proline-rich tyrosine kinase 2. J Biol Chem 1999;274:31863–31867. [PubMed: 10542211]
53. Tiede I, Fritz G, Strand S, Poppe D, Dvorsky R, Strand D, Lehr HA, Wirtz S, Becker C, Atreya R, Mudter J, Hildner K, Bartsch B, Holtmann M, Blumberg R, Walczak H, Iven H, Galle PR, Ahmadian MR, Neurath MF. CD28-dependent Rac 1 activation is the molecular target of azathioprine in primary human $CD4^+$ T lymphocytes. J Clin Invest 2003;111:1133–1145. [PubMed: 12697733]
54. Chernock RD, Cherla RP, Ganju RK. SHP2 and cbl participate in α-chemokine receptor CXCR4-mediated signaling pathways. Blood 2001;97:608–615. [PubMed: 11157475]
55. Inngjerdingen M, Torgersen KM, Maghazachi AA. Lck is required for stromal cell-derived factor 1 α (CXCL12)-induced lymphoid cell chemotaxis. Blood 2002;99:4318–4325. [PubMed: 12036857]
56. Okabe S, Fukuda S, Kim YJ, Niki M, Pelus LM, Ohyashiki K, Pandolfi PP, Broxmeyer HE. Stromal cell-derived factor-1α/CXCL12-induced chemotaxis of T cells involves activation of the Ras-GAP-associated docking protein p62Dok-1. Blood 2005;105:474–480. [PubMed: 15345598]
57. Park SY, Avraham H, Avraham S. Characterization of the tyrosine kinases RAFTK/Pyk2 and FAK in nerve growth factor-induced neuronal differentiation. J Biol Chem 2000;275:19768–19777. [PubMed: 10764815]
58. Avraham H, Park SY, Schinkmann K, Avraham S. RAFTK/Pyk2-mediated cellular signaling. Cell Signal 2000;12:123–133. [PubMed: 10704819]
59. Zanin-Zhorov A, Tal G, Shivtiel S, Cohen M, Lapidot T, Nussbaum G, Marqalit R, Cohen IR, Lider O. Heat shock protein 60 activates cytokine-associated negative regulator suppressor of cytokine signaling 3 in T cells: effects on signaling, chemotaxis, and inflammation. J Immunol 2005;175:276–285. [PubMed: 15972659]
60. Nobes CD, Hall A. Rho, rac, and cdc42 GTPases regulate the assembly of multimolecular focal complexes associated with actin stress fibers, lamellipodia, and filopodia. Cell 1995;81:53–62. [PubMed: 7536630]
61. Weiss-Haljiti C, Pasquali C, Hong J, Gillieron C, Chabert C, Curchod M, Hirsch E, Ridley AJ, van Huijsduijnen RH, Camps M, Rommel C. Involvement of phosphoinositide 3-kinase γ, Rac, and PAK signaling in chemokine-induced macrophage migration. J Biol Chem 2004;279:43273–43284. [PubMed: 15292195]
62. Nishita M, Aizawa H, Mizumo K. Stromal cell derived factor 1α activates LIM kinase 1 and induces cofilin phosphorylation for T-cell chemotaxis. Mol Cell Biol 2002;22:774–783. [PubMed: 11784854]

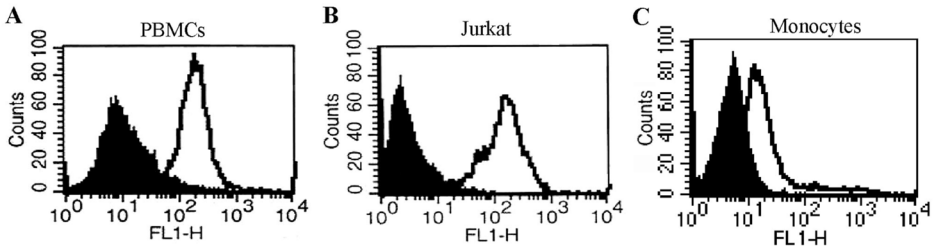

Fig. 1.

Expression of Robo. (A) PBMCs, (B) Jurkat T cells, or (C) monocytes were treated with Robo-1 (open area) or normal mouse IgG antibodies as a control (filled area) and stained with anti-mouse antibody conjugated with FITC. Cells were analyzed by flow cytometry.

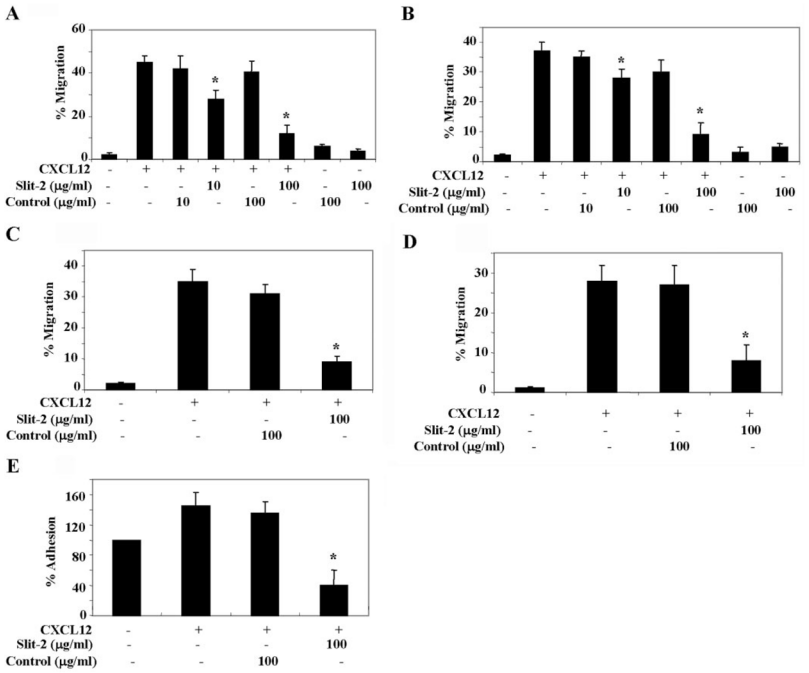

Fig. 2.

Slit-2 blocks the CXCL12-induced chemotaxis of T cells and inhibits transendothelial migration and cell adhesion. Jurkat T cells (A) and PBMCs (B) were pretreated with varying concentrations of Slit-2 supernatant (μg/ml) or control supernatant (μg/ml) and then subjected to a chemotactic assay in the presence of CXCL12 (50 ng/ml), as described in Materials and Methods. Jurkat T cells (C) and PBMCs (D) were pretreated with the indicated concentration of Slit-2 supernatant (μg/ml) or control supernatant (μg/ml) and then subjected to a CXCL12 chemotactic assay through a uniform monolayer of HUVECs, as described in Materials and Methods. (E) Jurkat T cells were treated with Calcein AM at 37°C for 30 min and monitored for their adhesive properties on the HUVEC monolayer in the presence of Slit-2 supernatant or control supernatant and CXCL12 (50 ng/ml) by using a cell adhesion assay kit. The percent cell adhesion was calculated by considering the OD of the untreated control as 100%. The experiments were done in triplicate and are presented as the mean ± SE. The data are representative of four different experiments. *, $P < 0.05$, for all experiments.

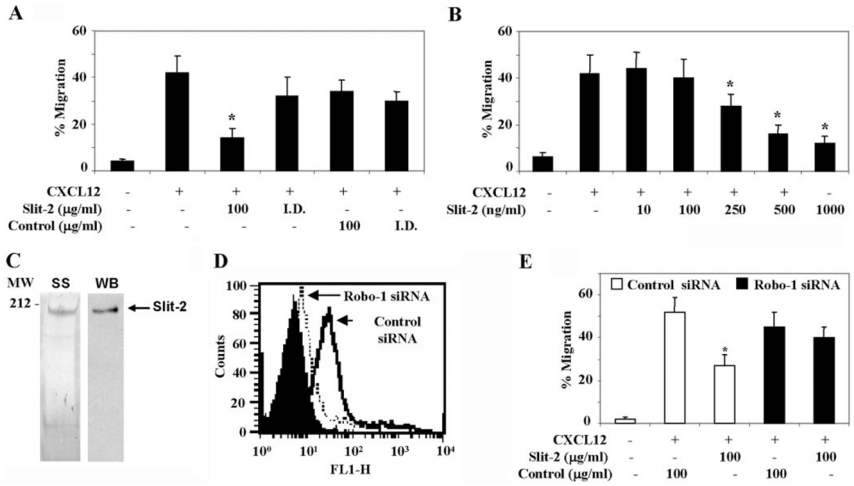

Fig. 3.

Slit-2/Robo-1 interaction inhibits CXCL12-induced chemotaxis. (A) The Slit-2 supernatant or control supernatant concentrates were incubated with anti-myc antibodies for 1 h at 4°C, followed by overnight incubation with protein A-Sepharose. The beads were removed by centrifugation, and the supernatant was used as the I.D. sample. Jurkat T cells were pretreated with the I.D. control supernatant (Control I.D., 100 μg/ml), I.D. Slit-2 supernatant (Slit-2 I.D., 100 μg/ml), or the undepleted supernatants (Slit-2 supernatant or control supernatant, 100 μg/ml). The cells were untreated (−) or treated (+) with CXCL12 as indicated and then subjected to chemotactic assays. (B) The Jurkat T cells were untreated (−) or pretreated with varying concentrations of FPLC-purified Slit-2 as indicated and then subjected to chemotactic assays using CXCL12 (50 ng/ml). (C) The purity of the FPLC-enriched Slit-2 was checked by Silver staining (SS) and by Western blot analysis (WB) using anti-myc antibody. (D) Control siRNA (solid line) and Robo-1 siRNA-transfected (dotted line) Jurkat T cells were stained using anti-Robo-1 antibody and analyzed by flow cytometry. Cells stained with control IgG (filled area) represent the antibody control. (E) Control siRNA and Robo-1 siRNA-transfected Jurkat T cells were pretreated with Slit-2 supernatant (100 μg/ml) or control supernatant (100 μg/ml) and then subjected to a chemotactic assay in the presence of CXCL12 (50 ng/ml), as described in Materials and Methods. The experiments were done in triplicate and are presented as the mean ± SE. The data are representative of four different experiments. *, $P < 0.05$, for all experiments

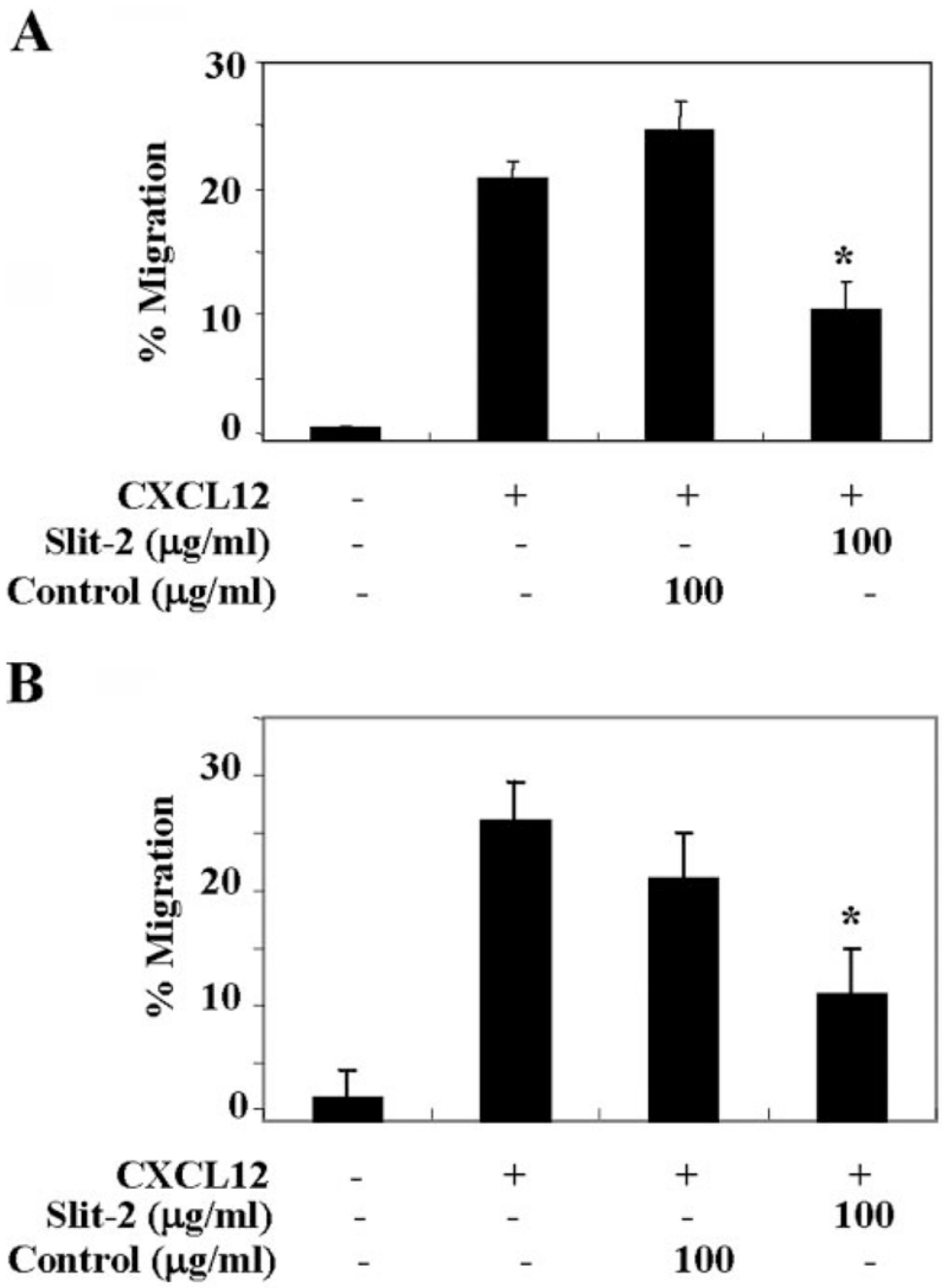

Fig. 4.

Slit-2 inhibits the CXCL12-induced chemotaxis of primary monocytes and $CD4^+$ T cells. Monocytes (A) and $CD4^+$ T cells (B) were isolated from peripheral blood by using negative selection kits according to the manufacturers' instructions (Dynal Biotech and StemCell Technologies). The cells were pretreated with Slit-2 supernatant (100 μg/ml) or control supernatant (100 μg/ml) and then subjected to chemotactic assays in the presence of CXCL12 (50 ng/ml), as described in Materials and Methods. The experiments were done in triplicate and are presented as the mean ± SE. The data are representative of four different experiments. *, $P < 0.05$.

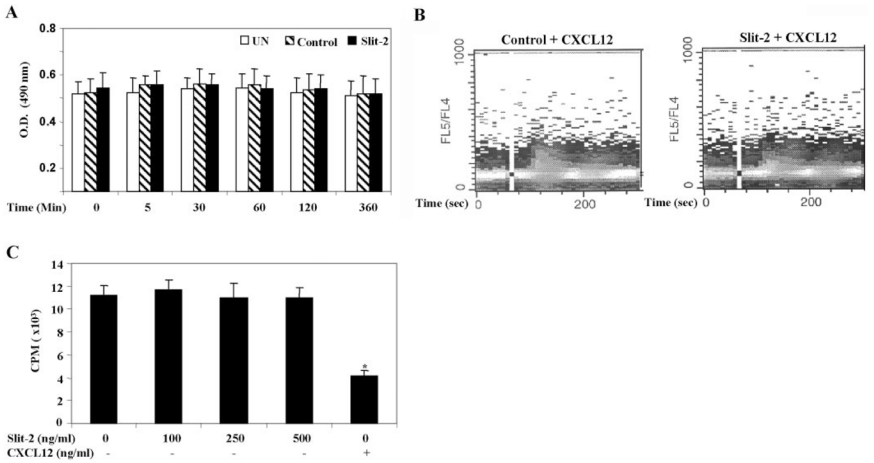

Fig. 5.

Slit-2 treatment does not cause cytotoxicity or inhibit CXCL12-induced calcium flux in Jurkat T cells, which were treated with Slit-2 supernatant (100 μg/ml) or control supernatant (100 μg/ml) for various time-points. (A) The number of viable cells was quantified by using the CellTiter 96® Aqueous kit (Promega), as per the manufacturer's instructions. UN, Untreated cells. (B) Slit-2 supernatant (100 μg/ml)-and control supernatant (100 μg/ml)-pretreated Jurkat T cells were loaded with Indo-1 AM and stimulated with CXCL12 (50 ng/ml). Calcium mobilization was then analyzed by flow cytometry, as described in Materials and Methods. Data are representative of three independent experiments. (C) The effect of Slit-2 on CXCL12 binding to CXCR4 was analyzed. Specifically, the binding of ^{125}I-labeled CXCL12 in the presence of various concentrations of purified Slit-2 or unlabeled CXCL12 (100 ng/ml) was determined in Jurkat T cells, as described in Materials and Methods. The experiments were done in triplicate and are presented as the mean ± SE. The data are representative of three different experiments. *, $P < 0.05$, for all experiments

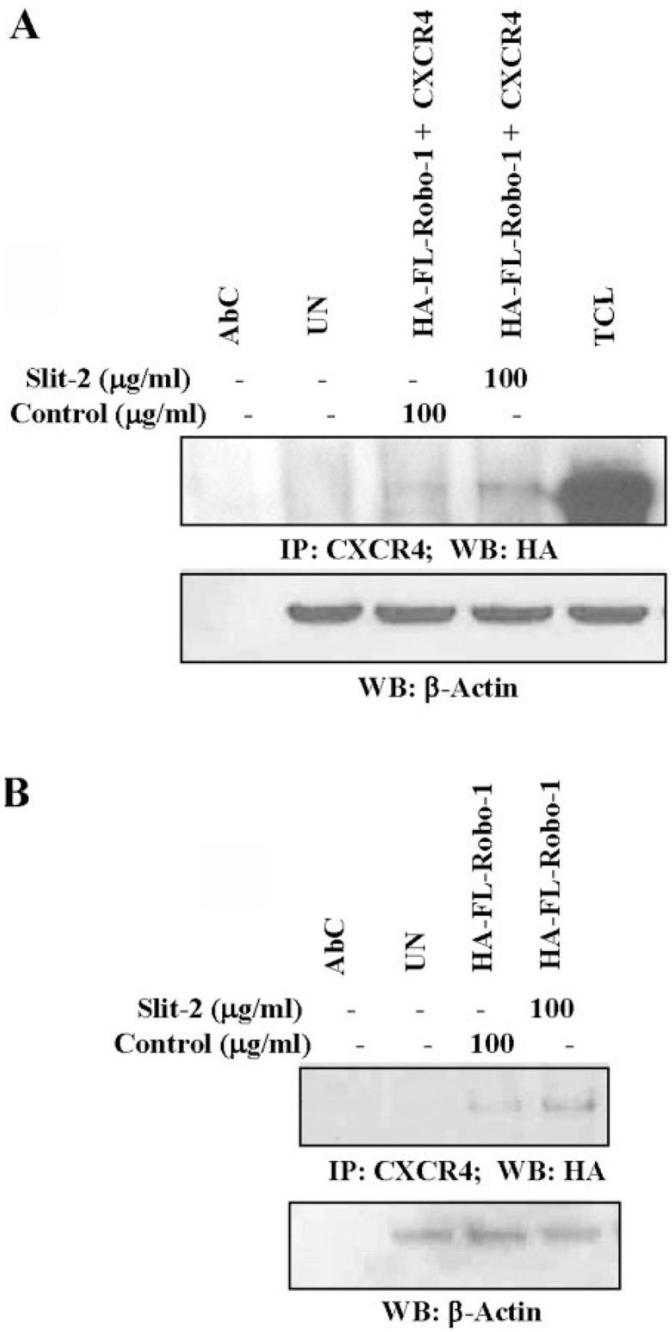

Fig. 6.

Slit-2 enhances the association between Robo-1 and CXCR4. (A) 293T cells were transfected with HA-FL-Robo-1 and FLAG-tagged CXCR4 plasmids by using Lipofectamine reagent (Invitrogen, Life Technologies), and (B) Jurkat T cells were transfected with HA-FL-Robo-1 by Nucleofection, according to the manufacturer's instructions (Amaxa Biosystems). These variously transfected cells were stimulated with Slit-2 supernatant (100 μg/ml) or control supernatant (100 μg/ml). The cell lysates were immunoprecipitated (IP) with anti-CXCR4 antibody and Western blotted with anti-HA antibody (A and B, upper panels). Equal protein was confirmed in each sample by Western blotting with anti-β-actin antibody (A and B, lower panels). AbC, Antibody control; TCL, total cell lysates; UN, untreated cells.

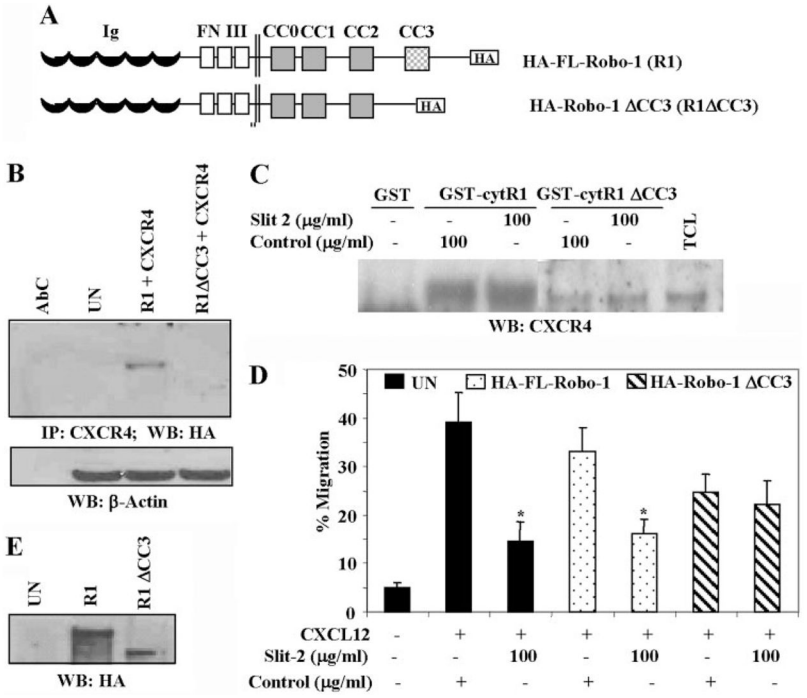

Fig. 7.

Role of the CC3 domain in the Robo-1 and CXCR4 association. (A) Schematic representation of HA-FL-Robo-1 (R1) and an HA-tagged mutant form of Robo-1 (Robo-1 with a deletion in the CC3 motif, HA-Robo-1 ΔCC3; R1ΔCC3). FN III, Fibronectin Type III repeats. (B) 293T cells were transfected with HA-FL-Robo-1 or HA-Robo-1 ΔCC3 as indicated, along with CXCR4 by using Lipofectamine reagent (Invitrogen, Life Technologies). These variously transfected cells were stimulated with Slit-2 cell-conditioned culture supernatant (100 μg/ml). The cell lysates were immunoprecipitated with anti-CXCR4 antibody and Western blotted with anti-HA antibody (upper panel). Equal protein was confirmed in each sample by Western blotting with anti-β-actin antibody (lower panel). (C) Jurkat T cells were stimulated with Slit-2 supernatant (100 μg/ml) or control supernatantμg/ml) for 30 min, and cell lysates were incubated with GST alone, with GST-cytR1, or GST-cytR1-ΔCC3 fusion proteins for 3 h at 4°C, after whicμl-immobilized glutathione resin (50% slurry) was added. Following a further incubation of 1 h at 4°C, the resin was washed, and the proteins were eluted in SDS sample buffer and analyzed by Western blotting with anti-CXCR4 antibody. (D) Jurkat T cells were transfected with HA-FL-Robo-1 or mutant Robo-1 (HA-Robo-1 ΔCC3) by using the Nucleofection method, stimulated with Slit-2 supernatantμg/ml) or control supernatantμg/ml) for 30 min at 37°C and then subjected to a chemotaxis assay toward CXCL12 (50 ng/ml), as described in Materials and Methods. *, $P < 0.05$. (E) Transfection efficiency in the Jurkat T cells was analyzed by Western blot analysis using anti-HA antibody. Experiments were repeated three times, and a representative one is shown. ABC, antibody control; UN, untreated cells; TCL, total cell lysates.

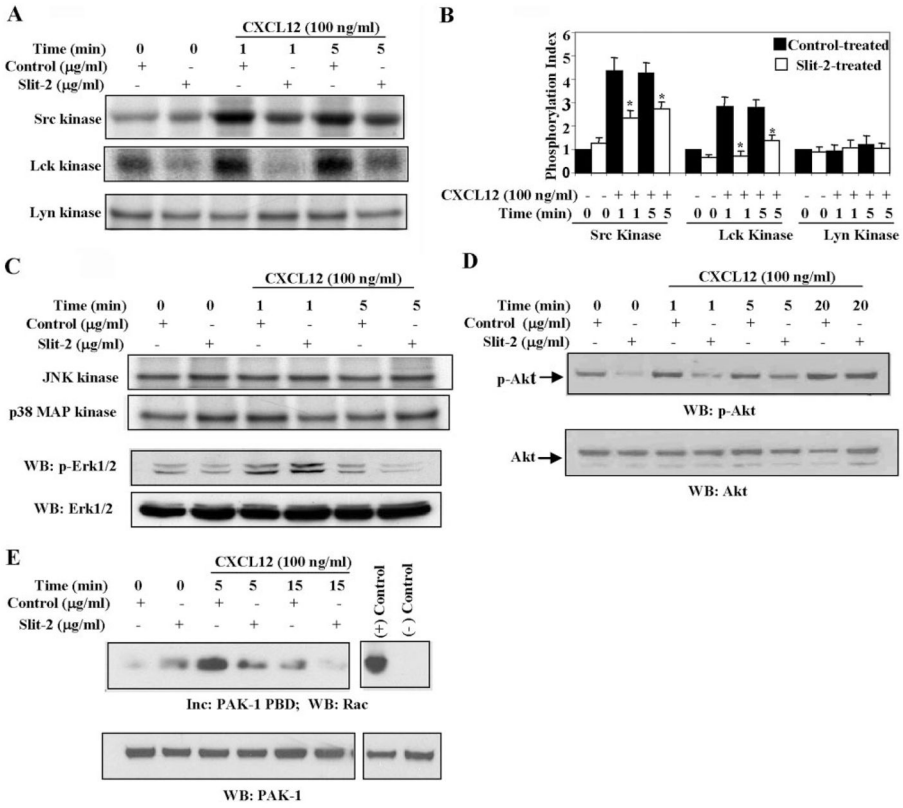

Fig. 8.

Effect of Slit-2 on the CXCL12-induced activities of Src kinase, MAPK, Akt, and Rac. (A) Jurkat T cells were preincubated with Slit-2 supernatant (100 μg/ml) or control supernatant (100 μg/ml) preparation and stimulated with CXCL12 (100 ng/ml) for the indicated time-points. The stimulated cells were lysed, and equal amounts of protein lysate were immunoprecipitated with Src kinase, Lck kinase, or Lyn kinase antibodies. The immune complexes were subjected to in vitro kinase assays as described in Materials and Methods. (B) Quantitative analysis of the protein phosphorylation of Src, Lck, and Lyn kinases. The band intensity in each lane was determined by densitometry. The phosphorylation index of each kinase shown in the bar graph was determined by calculating the value of each lane as the fold-increase over the unstimulated control (Control 0). *, $P < 0.05$. (C) Cell lysates were obtained from the Slit-2 supernatant (100 μg/ml)- or control supernatant (100 μg/ml)-pretreated Jurkat T cells after stimulation with CXCL12 (100 ng/ml) for various time periods. The lysates were immunoprecipitated with JNK kinase (top panel) or with p38 MAPK (second panel from top) antibodies and subjected to an in vitro kinase assay using c-Jun or MBP, respectively, along with labeled ATP as substrates. For the Erk1/2 assay, cell lysates were run on SDS-PAGE and Western blotted with phospho-Erk1/2 antibody (p-Erk1/2; second panel from bottom). The protein levels were monitored by stripping the blot and reprobing it with anti-Erk1/2 antibodies (bottom panel). (D) Slit-2 supernatant (100 μg/ml)- or control supernatant (100 μg/ml)-pretreated Jurkat T cells were unstimulated (0) or stimulated with CXCL12 (100 ng/ml) for the indicated time-points. The cells were lysed, and the lysates were analyzed by Western blotting with phospho-Akt antibody (p-Akt; upper panel). The blots were stripped and reprobed with anti-Akt antibody (lower panel). (E) Lysates from control and Slit-2 supernatant-treated cells in the presence of CXCL12 for various time periods were incubated with PAK-1 p21-binding domain (PBD) agarose. After incubation (Inc), the agarose beads were collected by centrifugation and analyzed for Rac-binding activity by Western blotting with anti-Rac mAb,

as described in Materials and Methods (upper panel). The protein levels were monitored by stripping the blot and reprobing it with anti-PAK-1 antibodies (lower panel). (+) Control, Cell lysate with GTPγ;S; (−) Control, cell lysate with GDPβS. All of the above experiments were repeated three times, and a representative one is shown.